INSTITUTE OF PHYSICS PUBLISHING NANOTECHNOLOGY
Nanotechnology **16** (2005) 1023–1028 doi:10.1088/0957-4484/16/8/004

Universal behaviour in the final stage of the breaking process for metal nanowires

Pavel Jelínek[1,2], **Rubén Pérez**[1], **José Ortega**[1] **and Fernando Flores**[1]

[1] Departamento de Física Teórica de la Materia Condensada, Universidad Autónoma de Madrid, E-28049, Spain
[2] Institute of Physics, Academy of Sciences of the Czech Republic, Cukrovarnická 10, 1862 53, Prague, Czech Republic

E-mail: pavel.jelinek@uam.es

Received 15 February 2005, in final form 5 April 2005
Published 12 May 2005
Online at stacks.iop.org/Nano/16/1023

Abstract
The gentle control of the nanometric distance between two materials has paved the way for the recent experimental studies on the formation and breaking of metal nanocontacts. In this work, the evolution of Al nanowires along the stretching process up to the final breaking is simulated with density functional calculations. This massive computational work involves the breaking of thick wires (with (111) and (100) orientations and 145 and 136 atoms respectively), and the influence of O, C and H impurities on their mechanical and electrical properties. These simulations show that, close to the breaking point, Al nanowires always develop a dimer geometry irrespective of the initial configuration, crystallographic orientation and the presence of point defects, explaining the universal behaviour of the force and the conductance found in the last stages of the stretching process in all the experiments.

M This article features online multimedia enhancements

In recent years, great progress has been achieved in understanding the conduction properties of matter at the atomic scale [1]. The formation and evolution of metallic nanocontacts have been studied in detail thanks to the gentle control of the distance at the nanometre scale provided by both the scanning tunnelling microscope (STM) [2] and the mechanically controllable break junction (MCBJ) [3]. Conductance measurements show the presence, during the elongation process, of discontinuous jumps in between regions of continuous evolution (plateaus), whose shape and average value are characteristic of the metal forming the contact [4]. The relation between the chemical valence and the electrical resistance was confirmed by the analysis of the final breaking stage (plateau) on nanocontacts where a superconducting state had been induced by the proximity effect. These experiments showed that each atomic contact can be uniquely characterized in terms of the number of channels and their transmission probabilities contributing to the conductance [5].

The simultaneous experimental characterization of the conductance and tensile forces along the stretching process [6] has been one of the most interesting results in the field: conductance and force jumps, that take place at the same stages, have been related to the irreversible (plastic) deformation of the nanowires to new stable structures. Conductance histograms, where the values of the conductance for thousands of different contacts are gathered, provide further evidence of the role of the nanowire geometry in the determination of the mechanical and electrical properties: the peaks in the histogram reflect the stable atomic configurations of the junction closely before breaking.

Understanding these quantum effects in the force and the conductance and predicting their evolution during the elongation process is not an easy task, as it requires three different key ingredients: the detailed knowledge of the nanocontact structure, a quantum mechanical calculation of the electronic properties associated with this geometry, and an accurate description of an intrinsically non-equilibrium phenomena as electronic transport. Most of the early work focused on the evolution of the nanocontact configuration, but the force fields [7, 8] and effective-medium theory potentials [9, 10] (fitted to reproduce bulk properties) used in these classical simulations severely limited their quantitative accuracy.

Predictive *ab initio* methods based in density functional theory (DFT) provide a reliable description of the electronic structure and the mechanical stability of the nanocontact. Alkali metal nanowires, thanks to their particularly simple electronic structure, have been amenable to a fully DFT structural calculation, where the 39 atoms of an Na nanowire were allowed to relax to their ground state configuration along the stretching process [11]. However, the computational cost for more realistic systems like Al, Au or Pd nanocontacts have confined the application of *ab initio* methods to the static analysis of some ideal geometries (single atom or short atomic chains in between pyramids or planes with the given nanocontact orientation) [12–17]. This approach, that includes a first-principles implementation of the Landauer formalism for the calculation of the conductance, has failed to reproduce basic experimental features of these nanocontacts close to the final breaking stage, like the characteristic increase in the conductance upon stretching in Al, or the value close to the conductance quantum $G_0 = 2e^2/h$ found systematically in the experiments irrespective of the orientation or initial conditions (for example, the theoretical conductance of a single atom contact between two (100) Al pyramids is $3G_0$ [15]).

These discrepancies between theory and experiment prompted our recent approach to the study of small (111)-oriented Al nanowires (with sizes ranging between 48 and 60 atoms), where we simulate, using a very efficient local orbital pseudopotential DFT approach (FIREBALL [18–20]), the evolution of the nanowire along the whole elongation process in order to get access to a realistic atomic configuration before the final breaking. Our simulations [21, 22] showed the correlation between discontinuous changes in the force (associated to changes in the bonding structure) and abrupt modifications of the conductance as the nanowires developed a thinner neck that, *in all the cases*, took the form of a dimer just before the breaking point.

Based on the success of this approach, that combines a direct access to a realistic structure of the nanocontact with a consistent and accurate determination of the transport properties based on the Keldish–Green function formalism (see [21–23]), we have performed large-scale simulations of the evolution of different Al nanowires (including up to 145 atoms) under tensile stress in order to assess the influence of size, crystallographic orientation and the role of defects (impurities like O, H and C) in the structure, mechanical response and conductance in the final stages of the nanowire deformation.

The information gathered on those systems yields a very rich and comprehensive picture of the plastic deformation of Al nanowires approaching their breaking point, where irrespective of the initial configuration and orientation, they all evolve to the same final dimer geometry that is responsible for the common conductance properties found before the breaking point in the experiments. Impurities do affect the mechanical response of the nanocontact but do not modify the final dimer geometry and the associated conductance properties.

In our calculations, we have addressed the influence of system size with the simulation of a (111)-oriented thick nanowire with 145 atoms, where results can be compared to our previous work on smaller nanocontacts with the same orientation [21, 22]. The initial configuration of the nanowire corresponds to the fcc stacking of five (111) planes with nine atoms per layer sandwiched between two Al(111)-surfaces, each simulated by two Al layers having a 5×5 periodicity in the direction parallel to the surface, that play the role of the two electrodes (see configuration A in figure 1(a)). In this case and all the following calculations, we also impose periodic boundary conditions in the direction perpendicular to the surface, joining artificially the last two layers (top and bottom in figure 1(a)): this means that each lead is effectively represented by four layers. The stretching of the system is simulated by increasing the distance between these two limiting layers by steps of 0.2 Å. After each step, the system is allowed to relax towards its ground state configuration, keeping fixed only the atoms in the two limiting layers (95 atoms are relaxed).

Figure 1 shows the total energy and the conductance of the nanowire along the stretching path and displays four selected snapshots of the nanowire geometry (points A–D). These configurations highlight the processes of layering, clustering and necking, leading to the dimer structure found in the last stages of the stretching process. The formation of additional (111) planes correlates with the energy jumps in figure 1(b) (e.g. six (111) planes are formed after the first energy jump around 2.4 Å). Significant modifications of the nanowire structure are confined to the three central layers of the initial relaxed configuration (case A), as shown by the labels 1–10 attached to the relevant atoms in figure 1.

Interestingly, the layering process that the nanowire undergoes from A to B is not symmetric: it results in two well-defined planes, having six and five atoms respectively, in the lower part, and the formation of a small cluster (including atoms 8 and 9), with a more complicated coordination, in the upper part. The necking process leading to structure C concentrates on those two lower layers (see atoms 1–7), while the upper cluster, more rigid as a result of plastic hardening, keeps its geometry practically unaltered. In configuration C, the nanowire has developed a small neck, defined by the atoms 3–5–10 on one side and the atoms 2–4–6 on the other. This structure is already close to the initial stages of the deformation of our thinner wires (see [21, 22]) and evolves in the same way, leading to the dimer formed by atoms 2 and 10 (see snapshot D) that defines the bond that is broken at the last stage of the deformation.

These similarities in the structure and deformation process in the stages prior to the final breaking for all the different (111)-oriented nanowires are also reflected in the differential conductance (figure 1(b)). The thicker nanowire reproduces the experimental conductance increase in the last plateau to a value close to G_0 [4] and the presence of three channels as measured in superconducting nanocontacts [5].

The role of the initial crystallographic orientation has been studied with a (100)-oriented nanowire formed by four layers with nine atoms each located between two Al(100)-surfaces, also simulated by two Al layers with a 5×5 periodicity (see case A in figure 2). This calculation involves 136 atoms, with 86 of them allowed to relax in the energy minimization procedure.

Deformation mechanisms differ significantly from those found in the (111)-nanowires in the first stages of the stretching process. The system favours a shear deformation where the two central layers change their stacking with respect to the

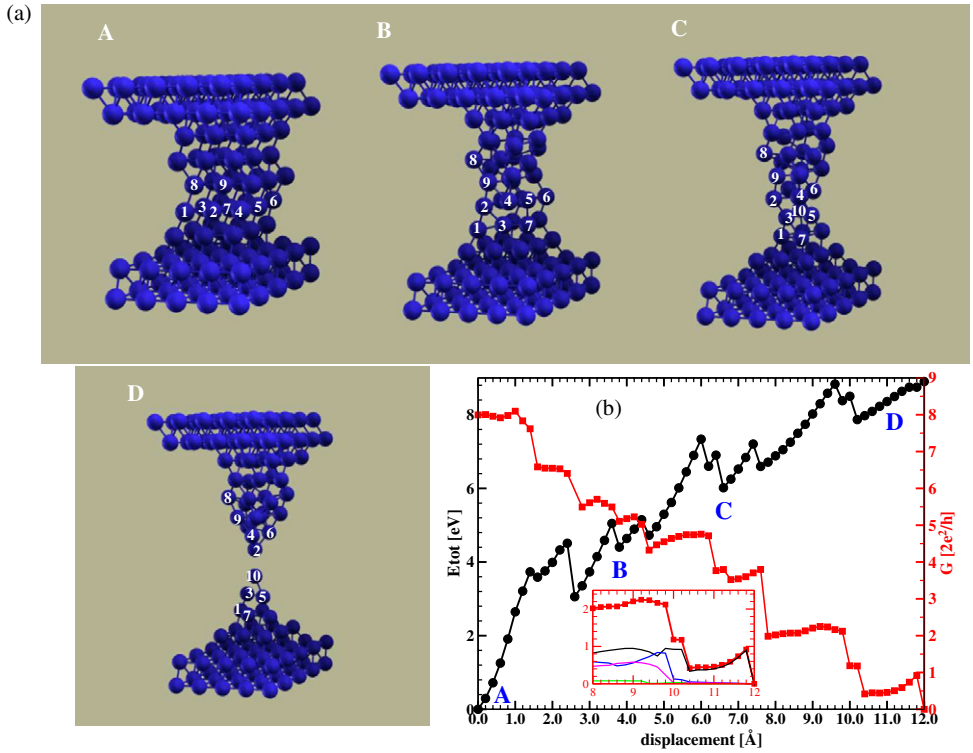

Figure 1. (a) Ball-and-stick model of the structure of the thick (111)-oriented Al nanowire for different steps of the stretching process. The atoms involved in some of the important bonding rearrangements related to discontinuous (A, B, C and D) changes in total energy, force and conductance are labelled 1–10. (b) Total energy (per unit cell, black circles) and total differential conductance (in units of the conductance quantum, red squares) of the Al-(111) nanowire as a function of the stretching displacement, Δd. The channels contributing to the conductance in the last stages of the breaking process are shown in the inset. See the multimedia file (movie 1) available at stacks.iop.org/Nano/16/1023.

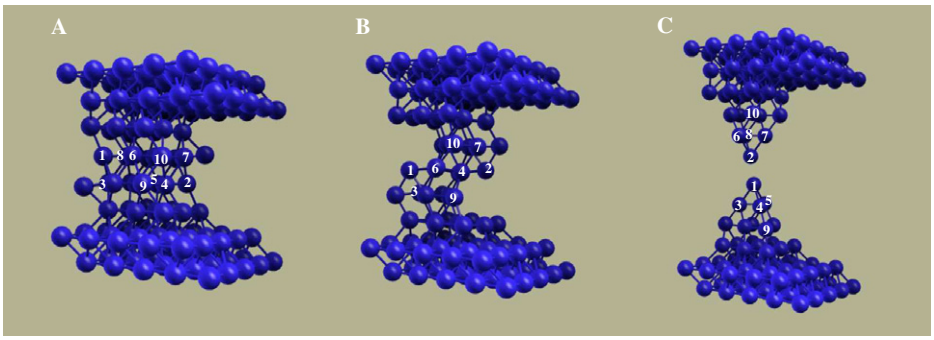

Figure 2. Ball-and-stick model of the structure of the thick (100)-oriented Al nanocontact showing selected relaxed atomic configurations along the stretching path. Frame A shows the initial geometry of the (100)-oriented Al nanocontact. Frame B represents a characteristic structure during the elongations process and frame C shows the final geometry of the nanocontact before the breaking point. The atoms involved in the neck formation are labelled 1–10 to illustrate their movement during the deformation process. See the multimedia file (movie 2) available at stacks.iop.org/Nano/16/1023.

outer layers of the nanowire with a rotation around the [100] direction, stretching and finally breaking some of their bonds (atoms 2, 4 and 5 with the layer underneath and atoms 1, 6 and 8 with the plane above). The final outcome of this process is the formation of three more compact (111) layers (with six atoms each) out of the original (100) planes (see configuration B in figure 2). Notice the inversion symmetry the nanowire keeps along the deformation path.

During the subsequent necking process, the nanowire deforms in a quite complicated way, involving also large displacements of certain atoms in the outer layers of the nanowire in the transition to a final structure that closely resembles two (111) pyramids. The last stages of deformation are thus defined by a dimer (atoms 1, 2 in configuration C), in similarity with the (111)-oriented nanowire.

In spite of the quite different deformation mechanisms that we have found for the nanowires with (111) and (100) orientations in the early stages of the stretching process, their structural evolution—in particular, the massive reorientation that takes place in the (100)-oriented nanowire—leads to a

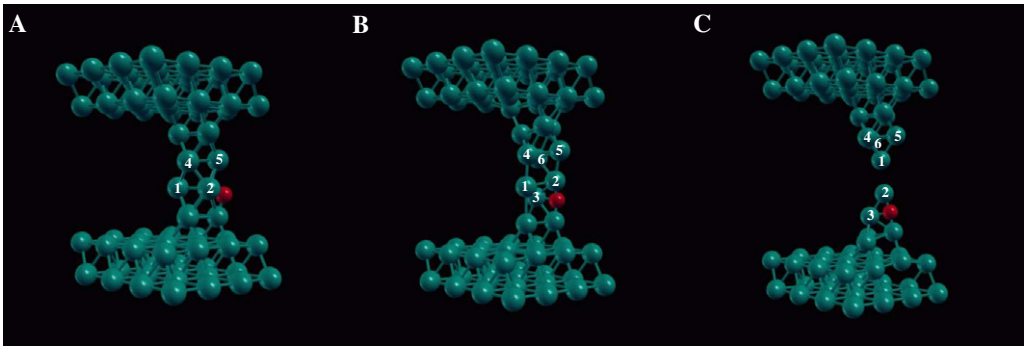

Figure 3. Ball-and-stick model of the structure of the thin (111)-oriented Al nanowire with an oxygen impurity (red atom) for different steps of the stretching process (configuration labels correspond to figure 4). The Al atoms involved in the important bonding rearrangements are labelled 1–6. See the multimedia file (movie 3) available at stacks.iop.org/Nano/16/1023.

common breaking geometry. This is defined by a dimer in agreement with the simulations calculated in previous works with a smaller number of atoms. This similarity is due to the behaviour of the (100) nanowire, that develops compact (111) layers in the initial stages of its deformation.

This same behaviour shows up in the evolution of the differential conductance along the stretching process. In the (111)-oriented nanowire (shown in figure 1(b)), its initial value is 8 $\frac{2e^2}{h}$ (with 16 channels contributing more than 0.1 G_0) and the system evolves with jumps of roughly $\frac{2e^2}{h}$ units (the number of channels being reduced by roughly three at each jump) until reaching the breaking point. The correlation between transport and structure makes the conductance of the (100)-oriented nanowire (not shown here) quite different from the (111) case in the early stages of the deformation process. The (100) nanowire starts with a different conductance of around 8.5 $\frac{2e^2}{h}$ with 18 channels contributing significantly (although the contact is also defined by planes with nine atoms) and does not show in its evolution the well defined plateaus displayed in figure 1(b). Conductance jumps are associated with the deformation processes that involve a significant modification of the neck effective area (see, for instance, configurations A and B in figure 2). However, both orientations show the same behaviour near the breaking point. In this limit the conductance shows the characteristic ascending plateau, that reaches the quantum of conductance $\frac{2e^2}{h}$ just before the final breaking, and has three channels contributing (see figure 1(b) for the (111)-oriented nanowire). The dominant channel is associated to the σ-bond formed between the sp^3-orbitals of the Al dimer, while the other two minority channels are associated with π-bonds. The robust conductance quantization seen in the experiments is thus associated with the mechanical stability of the dimer configuration that characterizes the last stages of the deformation process in both nanowires.

Finally, we have assessed the influence of a relevant external factor, the presence of isolated impurities from likely contaminants, on the final stages of the nanowire breaking process. For that purpose, we have studied the changes induced by the presence of single atoms of O, H and C on the evolution of a (111)-oriented Al nanowire, with four layers of three atoms between (111)-Al surfaces with 4 × 4 periodicity. The independence of the basic results on system size found for the clean (111) nanowires justifies the use of this smaller system.

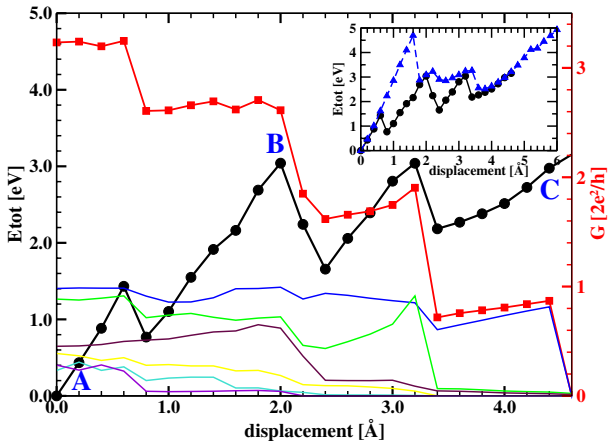

Figure 4. Total energy (per unit cell, black circles), total differential conductance (in units of the conductance quantum, red squares), and contribution of the different channels to the conductance for the thin (111)-oriented Al nanowire with an oxygen impurity (for detailed atomic geometries see figure 3) as a function of the stretching displacement, Δd. The inset shows the influence of the oxygen impurity on the mechanical response, comparing the evolution of the total energy of the clean (blue triangles) and oxygen-contaminated (black circles) nanowires.

Oxygen has a dramatic influence on the mechanical properties of the nanowire, inducing a more brittle behaviour that shortens by 25% the maximum displacement before breaking and reducing significantly the elastic behaviour of the nanowire (see the inset in figure 4). Configuration A in figure 3 corresponds to the initial relaxed geometry. The O atom is coordinated with three Al atoms, with distances around 1.90 Å, and does not introduce a significant distortion in the topology of the structure compared to the clean nanowire. However, the evolution of the system upon stretching is quite different. Case B shows the geometry after a displacement of 2 Å. At variance with the clean nanowire, the deformation is not confined to the two central layers (atoms (4, 5, 6) and (1, 2, 3) in figure 3) but there is a significant strain in the bonds between the wire and the lower lead. Notice that O is still coordinated with the same three atoms of the initial configuration A. This is the key factor in explaining the embrittlement: oxygen keeps atoms 2 and 3 strongly bonded to the layer underneath, in such

a way that along the stretching process the atom 1 (of the 1, 2, 3-layer) suffers the largest deformation. This process is fully developed in configuration C (figure 3), where a compact structure has been formed in the upper part of the wire and atom 1 is now forming the 1–2 dimer that defines the neck of the nanowire just before its breaking. Calculations for other initial locations of the impurity show that the dimer is always formed next to the oxygen atom. In a clean nanowire only atom 3 remains bonded to the layer underneath, while atoms 1 and 2 are displaced upwards, giving rise to an elongated structure, with the final dimer of the neck formed by atoms 2 and 3, that is able to sustain a larger strain before the final breaking (see the multimedia files available at stacks.iop.org/Nano/16/1023).

In spite of the different evolution induced by the effect of O in the specific motion of certain atoms in the nanowire, it is important to realize that the system has also developed at the breaking point a dimer structure, very much in similarity with the results found for all the clean nanowires (see figures 1 and 2). This geometry leads to the conductance behaviour (figure 4) that we have also found in the cases of figures 1 and 2 for the last stage of the nanowire stretching. The conductance presents a positive slope as a function of the stretching deformation and we also find the same behaviour of the conductance channels along the last plateau with one dominant channel out of three. The maximum conductance, before the breaking, is close to 0.9 $\frac{2e^2}{h}$, a little lower than the results found for the clean nanowires.

Similar calculations for an isolated H impurity show that H does not significantly affect the properties of the clean nanowire. No major differences are found in both the initial relaxed configuration (similar to case A in figure 3) and the subsequent evolution, leading to a final dimer structure (that is formed far away from the impurity) with the same conductance behaviour and a maximum value slightly lower than the conductance quantum. The effect of the C impurity is intermediate between those of H and O. C strongly bounds to the Al atoms, distorting even the initial relaxed configuration compared to the clean nanowire, and affects the details of the deformation process, but the maximum elongation before the final breaking is not very different from that of the clean nanowire, with the impurity far away from the dimer that defines the final Al neck. The conductance along the last stages of the stretching path evolves similarly to all the previous cases: three open channels (one dominant) appear on the last plateau and near the breaking point the conductance has a value close to $\frac{2e^2}{h}$.

Finally, we comment on the evolution of the force upon stretching for the different nanowires. They can be calculated theoretically as a derivative of the total energy versus displacement curves like the one shown in figure 1(b) for the thick (111)-oriented nanowire. The force shows discontinuous changes that are coincident with the conductance jumps, in agreement with the experiments. The detailed evolution depends on the particular nanowire considered, but as a general trend the total force on the elastic regions correlates with the cross section of the nanowire, although the force per atom in the neck increases as the neck area is reduced. For instance, from the data in figure 1(b) for the (111)-oriented nanowire, the maximum force is ∼4.9 nN (∼0.55 nN/atom), while near the breaking point its value is ∼1.02 nN. A similar trend is found in the (100)-nanowire, with maximum force ∼6.1 nN (∼0.7 nN/atom), and 1.03 nN at the breaking point, showing, in spite of the initial differences, the common behaviour of the force in the last stages of the breaking process for both orientations. In the case of the thinner (111)-nanowire, the presence of the O impurity (figure 4) reduces the maximum value of the force in the elastic region by 17%, but both systems present an almost identical force close to the breaking point.

In conclusion, we have presented large-scale first-principles calculations simulating the plastic deformation of Al nanowires near the final stage of their breaking process. Our calculations show that the Al nanowires present a universal behaviour in their mechanical deformation and electrical conductance irrespective of their initial geometrical configuration, crystallographic orientation and the presence of impurities. In all our simulations, we have found that, close to the breaking point, Al nanowires always develop a dimer geometry. This dimer structure reproduces the relevant experimental findings: the characteristic final ascending plateau, reaching a value close to the conductance quantum, $\frac{2e^2}{h}$, and the presence of three contributing channels. The robust conductance quantization and the universal behaviour of the force near the breaking point are thus associated with the mechanical stability of the dimer configuration that characterizes the last stages of the deformation process in the Al nanowires.

Acknowledgments

PJ gratefully acknowledges financial support by the Ministerio de Educacion y Ciencia of Spain. This work has been supported by the European Union (project no. HPRN-CT-2000-00154) and the DGI-MCyT (Spain) under contracts MAT2001-0665 and MAT2002-01534.

References

[1] Agräit N, Levy-Yeyati A and van Ruitenbeek 2003 *Phys. Rep.* **377** 81–279
[2] Rubio-Bollinger G, Agräit N and Vieira S 1996 *Phys. Rev. Lett.* **76** 2302–5
[3] Scheer E, Joyez N, Esteve D, Urbina C and Devoret M H 1997 *Phys. Rev. Lett.* **78** 3535–8
[4] Cuevas J C *et al* 1998 *Phys. Rev. Lett.* **81** 2990–3
[5] Scheer E *et al* 1998 *Nature* **394** 154–7
[6] Rubio-Bollinger G, Bahn S R, Agräit N, Jacobsen K W and Vieira S 2001 *Phys. Rev. Lett.* **87** 026101
[7] Landman U, Luedtke W D, Salisbury B E and Whetten R L 1996 *Phys. Rev. Lett.* **77** 1362–5
[8] Todorov T N and Sutton A P 1993 *Phys. Rev. Lett.* **70** 2138–41
[9] Bradkovsky A M, Sutton A P and Todorov T N 1995 *Phys. Rev.* B **52** 5036–51
[10] Sörensen M R, Brandbyge M and Jacobsen K W 1998 *Phys. Rev.* B **57** 3283–94
[11] Nakamura A, Brandbyge M, Hansen L B and Jacobsen K W 1999 *Phys. Rev. Lett.* **82** 1538–41
[12] Taraschi G, Mozos J-L, Wan C C, Guo H and Wang J 1998 *Phys. Rev.* B **58** 13138
[13] Mehrez H *et al* 2002 *Phys. Rev.* B **65** 195419
[14] Brandbyge M, Mozos J-L, Ordejon P, Taylor J and Stokbro K 2002 *Phys. Rev.* B **65** 165401
[15] Palacios J J, Perez-Jimenez A J, Louis E, San-Fabian E and Verges J A 2002 *Phys. Rev.* B **66** 35322

[16] Heurich J, Cuevas J C, Wenzel W and Schön G 2002 *Phys. Rev. Lett.* **88** 256803
[17] Di Tolla 2000 *Surf. Sci.* **454–456** 947
[18] Demkov A A, Ortega J, Sankey O F and Grumbach M P 1995 *Phys. Rev.* B **52** 1618–30
[19] Lewis J P, Glaesemann K R, Voth G A, Fritsch J, Demkov A A, Ortega J and Sankey O F 2001 *Phys. Rev.* B **64** 195103
[20] Jelínek P, Wang H, Lewis J P, Sankey O F and Ortega J 2005 *Phys. Rev.* B accepted (*Preprint* cond-mat/0409509)
[21] Jelínek P, Pérez R, Ortega J and Flores F 2003 *Phys. Rev.* B **68** 085403
[22] Jelínek P, Pérez R, Ortega J and Flores F 2004 *Surf. Sci.* **566–568** 13
[23] Mingo N *et al* 1996 *Phys. Rev.* B **54** 2225